Journal of Engineering Science and Technology
Vol. 8, No. 1 (2013) 69 - 76

INVESTIGATING SPOT WELD GROWTH ON 304 AUSTENITIC STAINLESS STEEL (2 mm) SHEETS

NACHIMANI CHARDE*, RAJPRASAAD RAJKUMAR

Department of Mechanical, Material and Manufacturing Engineering
The University of Nottingham–UK, Malaysia Campus,
Jalan Broga, 43500 Semenyih, Selangor Darul Ehsan, Malaysia
*Corresponding Author: dr.nachimani@yahoo.com

Abstract

Resistance spot welding (RSW) has revolutionized automotive industries since early 1970s for its mechanical assemblies. To date one mechanical assembly out five is welded using spot welding technology in various industries and stainless steel became very popular among common materials. As such this research paper analyses the spot weld growth on 304 austenitic stainless steels with 2mm sample sheets. The growth of a spot weld is primarily determined by its parameters such as current, weld time, electrode tip and force. However other factors such as electrode deformations, corrosions, dissimilar materials and material properties are also affect the weld growth. This paper is intended to analyze only the effects of nuggets growth due to the current and weld time increment with constant force and unchanged electrode tips. A JPC 75kVA spot welder was used to accomplish it and the welded samples were undergone tensile test, hardness test and metallurgical test to characterize the formation of weld nuggets.

Keywords: Spot welding, Nugget growth, Stainless steel spot welding.

1. Introduction

Spot welding process is a joining process in which two or more metal sheets are joined together through fusion at a certain point [1]. The spot welder uses two copper electrodes to press the work sheets together and force high current to pass through it. The growth of weld nugget is therefore determined by its controlling parameters such as the current, weld time, electrode tips and electrode force [2]. In this experiment the current and weld time were varied to see the weld growth while the electrode tips and force remained unchanged [3]. The investigation was carried out to characterize the spot weld growth for 2 mm base metals by varying the welding current and weld time, in other word.

2. Experimentation

The rectangular-shaped specimens were equally prepared with a size of 200mm (length) × 25 mm (width) × 2 mm (thickness) as shown in the Fig. 1 and its chemical composition is listed in Table 1. Initially some samples were welded to characterize the working regions without producing expulsion or poor weld. Hence it was found that the welding current of 7, 8, 9 kA and weld time of 10, 15, 20 cycles were simply giving reasonable working region and therefore a weld schedule was developed in accordance with these values (Table 2). Meanwhile the electrode force was set to be constant at 3 kN and truncated type electrode tips (diameter 5 mm) were also kept unchanged.

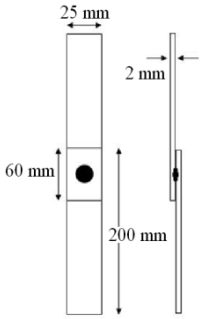

Fig. 1. Welding Sample with Dimension.

Table 1. Chemical Composition of 304 Austenitic Stainless Steel.

Element	C	Cr	Ni	Mn	Si	S	N	P
Weight %	0.046	18.14	8.13	1.205	0.506	0.004	0.051	0.030

Table 2. Weld Schedule.

Weld Schedule	Sample No	Material	Electrode Tip (mm)	Current (kA)	Time (cycle)	Force (kN)
1	1-5	SS	5	6	10	3
2	6-10	SS	5	7	10	3
3	11-15	SS	5	8	10	3
4	16-20	SS	5	6	15	3
5	21-25	SS	5	7	15	3
6	26-30	SS	5	8	15	3
7	31-35	SS	5	6	20	3
8	36-40	SS	5	7	20	3
9	41-45	SS	5	8	20	3

A pair of water cooled copper-alloy electrodes with truncated tips was used to join these base metals. The test samples were initially placed on the top of lower electrode (tip) of the spot welder (75 kVA) as overlaying 60 mm on each other and then the initiating pedal was pressed. The weld process was started right after with squeezing cycles and; once the squeezing force is reached the welding current is delivered in accordance with the given preset values. Thereafter the electrode pressing mechanism (pneumatic based) consumes some time for cold work and eventually return to the home position of electrode. The process controlling parameters (welding current and weld time) are set before the welding process starts. So the weldment happens in accordance with these parameters.

3. Results and Discussion

Hardness test was carried out by using Rockwell hardness (B Scale) machine with 20 kg of pressing forces on selected 9 samples from weld schedule (Fig. 2). The hardness of welded areas (≈ 96 HRB) seemed to be higher than unwelded areas (≈ 86 HRB) due to the solidification process. However the hardness distribution along the line of measurements was not giving any relationship as it fluctuates up and down at fusion zones [4]. Moreover the heat affected zones (≈ 90 HRB) was lower in hardness as compared to fusion zones; as it was partially melted but not fully.

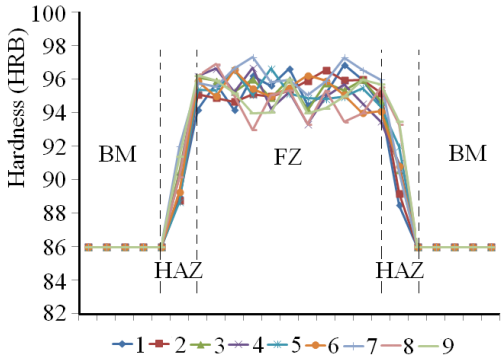

Fig. 2. Hardness Survey.

The ultimate tensile strength (UTS) at which the maximum breaks occur was taken into consideration using tensile machine for all the samples [5]. Five samples were developed for each weld schedule and the average values of five samples were taken as final tensile strength as shown in Fig. 3. The first five samples show the real tensile test values and consecutive sixth bar shows the average that obtained. As for the weld schedule from 1 to 2; there are increases in strength due to increase in current (7 kA to 8 kA) with time cycle 10. The same principle goes to weld schedule 2 to 3 as another increase in current (8 kA to 9 kA) was applied whilst the time cycle was same as before [6]. Similar results were notice for weld schedule 4, 5, 6 and 7, 8, 9. Besides the weld time increments from weld schedule 1 to 4 and from 4 to 7 with same current were also produced increase in strength. Further analysis of weld time increment of 2, 5, 8 and 3, 6, 9 also produced similar result [7]. In contrast, expulsion had caused inconsistent weld development and therefore extreme cases were not analyzed here. However some common types of tensile break were found through this experiment as shown in Table 3. Having considered the failure modes of tensile test, we have noticed some of the common failure while performing tensile test. Thus: (A) represents Interfacial Fracture regions of base metals. The failure mode (B) represents Tear from Edge of one side of base metals and (C) represents Tear from Edge of both sides of base metals (Fig. 4).

The standard metallurgical study was conducted for each weld schedule out of nine. It obviously shows how the nuggets growths were happened in 304 austenitic stainless steel with respect to current and weld time changes. It particularly shows the diameter of fusion zones (FZ), heat affected zones (HAZ), indentation of electrode (IE), and micro structural view of after the solidification (Fig. 5) [8]. The strengths were increased due to diameter increment but the hardness increments

happened due to solidification. For an instance, when the weld time is increased from 10 to 15 and from 15 to 20 cycles; the welded areas were given sufficient time to melt and therefore the nugget diameters were increased (From 4.669 mm to 5.757 mm and from 5.757 mm to 6.301 mm). These changes have been graphically shown in Table 4, column 1. Likewise when the currents were increased from 7 to 8 and from 8 to 9 kA; the welded areas were, therefore given more current to pass through and consequently more heat was generated. This is how the diameters were also correspondingly increased when the welding current was increased. These have been graphically shown in Table 4, column 2.

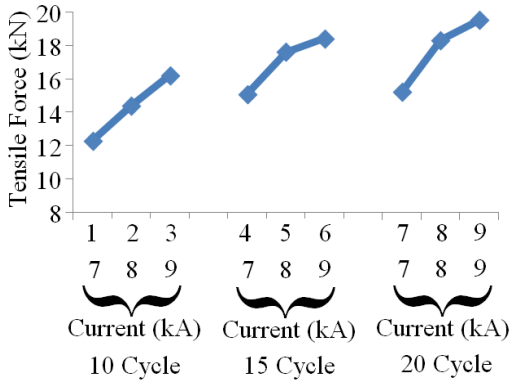

Fig. 3. Tensile Test Result.

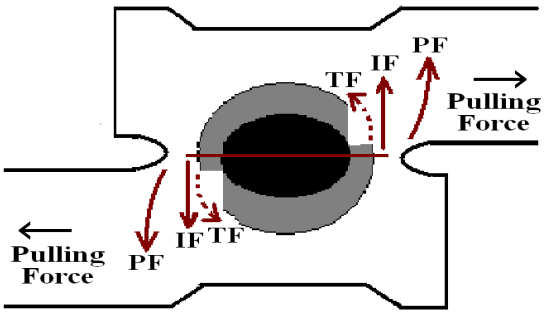

Fig. 4. Failure Modes of Tensile Test.

Table 3. Common Breaks of Tensile Test.

		
Button Pull Out (6 kA, 20 Cycle)	Tear from One Side Weld (7 kA, 20 Cycle)	Tear from both Side Weld (8 kA, 20 Cycle)

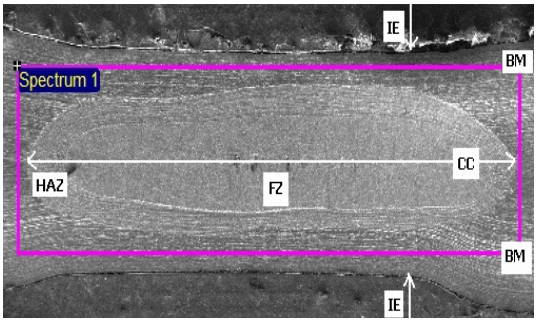

Fig. 5. Weld Zones of 304 Austenitic Stainless Steels.

Table 4. Macro Graph of 304 Austenitic Stainless Steels.

Column 1 (Weld Time Increments)	Column 2 (Current Increments)
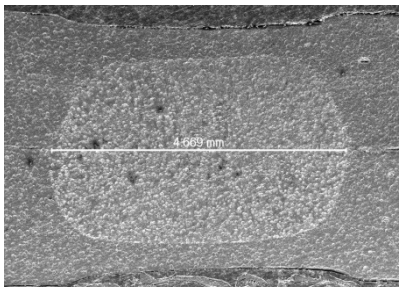 (10 Cycles – 4.669 mm)	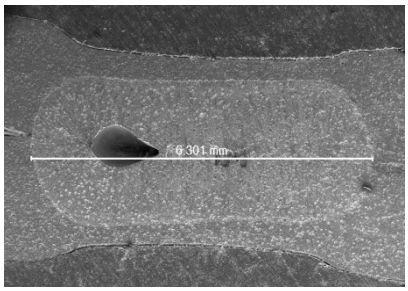 (Current 7 kA – 6.301 mm)
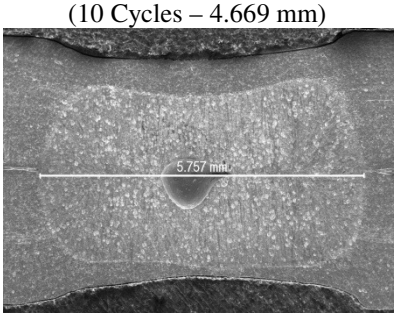 (15 Cycles – 5.757 mm)	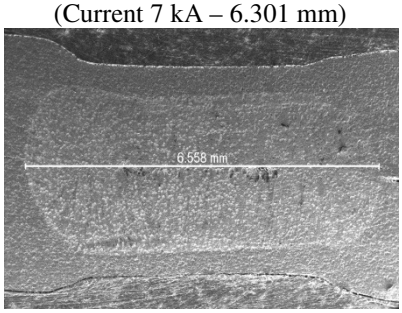 (Current 8 kA – 6.558 mm)
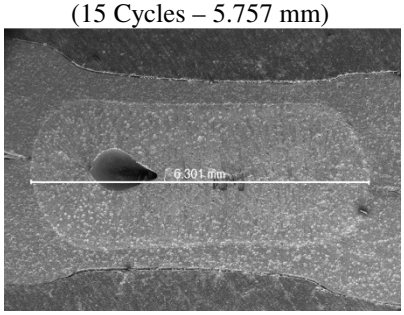 (20 Cycles – 6.301 mm)	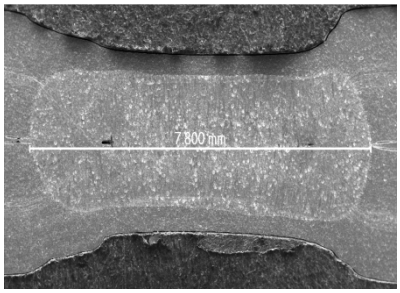 (Current 9 kA –7.800 mm)

The energy-disperse x-ray (EDX) detection was conducted to differentiate the chemical composition of the base metal at the welded and unwelded areas. Figures 6 and 7 are showing the EDX test result for 304 austenitic stainless steel (2 mm sheets). The results are showing that the chromium to nickel ratio was increased so more ferrite phases were induced at the welded zones. It can be said in another word, that the vermicular and lathy ferrite increases during welding process and resulted skeleton outlook at the welded zones as compared to unwelded zones [9].

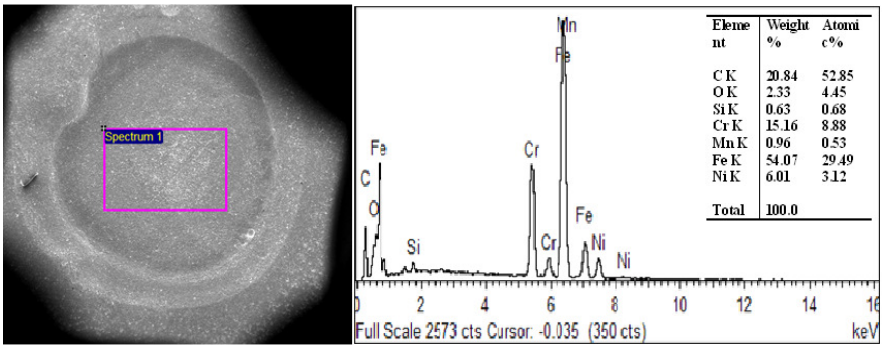

Fig. 6. Chemical Properties at the Fusion Zones.

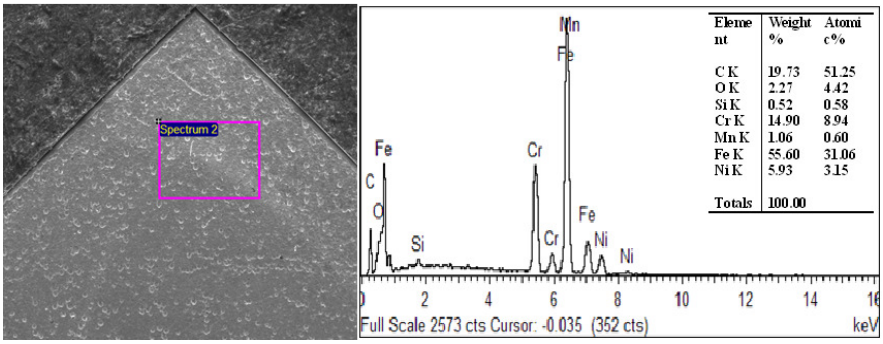

Fig. 7. Chemical Properties at the Base Metal.

The Schaeffler diagram (Fig. 8) prediction is the basic methods of predicting the phase balances in stainless steel welds. By getting the right intersecting coordinate of nickel and chromium; the phase balances after the welding process is obtainable. The nickel equivalent composition is calculated for the austenite stabilising elements and the chromium equivalent composition is calculated for ferrite stabilising elements. These two components show the compositional equivalent areas where the phases of austenite (A), ferrite (F), martensite (M) (and/or mixtures of these three components) have been formed. The red colour star represents the unwelded region (M+F regions) whereas the blue colour star represents the welded region (A+M+F regions) in which the ferritic properties became rich due to welding process. The general effect of cold work is to increase the yield strengths; increase the hardness and decrease the elongation [10].

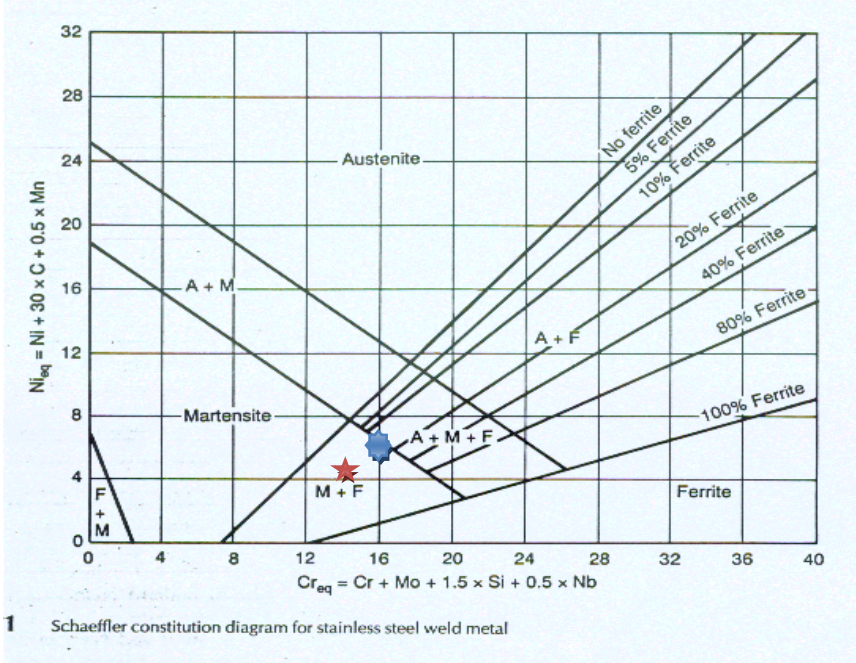

Fig. 8. Schaeffler Constitutional Diagram.

4. Conclusions

This paper looks into the spot weld growth on 304 austenitic stainless steel with 2 mm thickness sheets and it is concluded that:

- Hardness of welded zones is greater than the hardness of the un-welded zone and also the heat affected zones.
- The welding current and weld time increments have resulted diameters increment at the welded zones.
- Tensile forces have proportional relationship with current and weld time increaments until the expulsion limit occurs.
- The common three failure modes were seen as the poor weld produces an interfacial fracture (IF); the medium weld produces tear form one side (PF); and a good weld produces button pullout or tear from both sides (TF).
- Chromium to nickel ratio has been increased due to welding process and therefore the ferritic properties became rich at the welded zones.

Acknowledgement

We would like to thank Ministry of Science, Technology and Innovation, Malaysia (MOSTI) for their financial support during the experiment. This research paper is part of Nachimani Charde's PhD award.

References

1. Maa, C.; Chena, D.L.; Bhole, S.D; Boudreau, G.; Lee, A.; and Biro, E. (2008). Microstructure and fracture characteristics of spot-welded DP600 steel. *Materials Science and Engineering A*, 485(1-2), 334-346.
2. Özyürek, D. (2008). An effect of weld current and weld atmosphere on the resistance spot weld ability of 304L austenitic stainless steel. *Materials and Design*, 29(3), 597-603.
3. Sun, D.Q.; Lang, B.; Sun, D.X.; and Li, J.B. (2007). Microstructures and mechanical properties of resistance spot welded magnesium alloy joints. *Materials Science and Engineering A*, 460-461, 494-498.
4. Yang, HG.; Zhang, YS.; Lai, XL.; and Chen, G. (2008). An experimental investigation on critical specimen sizes of high strength steels DP600 in resistance spot welding, *Materials and Design*, 29(9), 1679-1684.
5. Von Maubeuge, K.P.; and Ehrenberg, M. (2000). Comparison of peel bond and shear tensile test methods for needle punched geo synthetic clay liners. *Geotextiles and Geomembranes*, 18(2-4), 203-214.
6. Kahraman, N. (2007). The influence of welding parameters on the joint strength of resistance spot-welded titanium sheets. *Materials and Design*, 28(2), 420-427.
7. Marashi, P.; Pouranvari, M.; Amirabdollahian, S.; Abedi, A.; and Goodarzi, M. (2008). Microstructure and failure behaviour of dissimilar resistance spot welds between low carbon galvanized and austenitic stainless steels, *Materials Science and Engineering A*, 480(1-2), 175-180.
8. Qiu, R.; Satonaka, A.; and Iwamoto, C. (2009). Effect of interfacial reaction layer continuity on the tensile strength of spot welded joints between aluminum alloy and steels. *Materials and Design*, 30(9), 3686-3689.
9. Shamsul, J.B.; and Hisyam, M.M. (2007). Study of spot welding of austenitic stainless steel type 304. *Journal of Applied Sciences Research*, 3(11), 1494-1499.
10. Oikawa, H.; Murayama, G.; Sakiyama, T.; Takahashi, Y.; and Ishikawa, T. (2007). Resistance spot weldability of high strength steel (HSS) sheets for automobiles. *Nippon Steel Technical Report*, No. 95.